◎ 논 문
◎ Original Paper

DOI: http://dx.doi.org/10.5293/kfma.2016.19.4.019
ISSN (Print): 2287-9706

CFD Analysis of Natural Convection Flow Characteristics of Various Gases in the Spent Fuel Dry Storage System

Doyoung Shin* · Uiju Jeong* · Gyoodong Jeun* · Sung Joong Kim*†

Key Words : Backfill Gas(충전기체), CFD Analysis(전산유체역학 분석), Dry Storage System(건식저장시스템), Natural Convection (자연대류), Spent Fuel(사용후핵연료)

ABSTRACT

Objective of this study is to compare the inherent characteristics of natural convection flow inside the canister of spent fuel dry storage system with different backfill gases by utilizing computational fluid dynamics (CFD) code. Four working fluids were selected for comparison study. Helium currently used backfill gas for canister, air, nitrogen, and argon are frequently used as coolant in many heat transfer applications. The results indicate that helium has very distinct conductive behavior and show very weak natural convective flow compared to the others. Argon showed the strongest natural convective flow but also the worst coolability. Air and nitrogen showed similar characteristics to each other. However, due to difference in Prandtl number, nitrogen showed more effective natural convective flow. These results suggest that experimental validation for the nitrogen is needed to investigate the potential coolability other than currently commercially used helium.

1. Introduction

Nuclear power plants (NPPs) have played important role in generating electricity with excellent efficiency and reliability compared to conventional resources such as fossil fuels, wind, and tidal power over the last few decades. Fresh nuclear fuels are burned up in the pressurized water reactor for about 54 months and are discharged. The discharged fuels, also known as spent fuels are inevitably highly radioactive while utilizing nuclear power. Even after the discharge, the spent fuels keep generate high-level radiations and considerable heat due to decay of fission fragments such as I-131 and Cs-137. Although the decay heat is very small compared to full operation power, it is high enough to cause failure of the fuel cladding, which leads to radioactive nuclide release into the environment unless sufficient cooling is provided. Therefore, necessity of spent fuel interim storage system was emphasized to decrease radiation level and heat generation before the permanent disposal or recycling.

There are two ways of interim storage for the spent fuels. One is wet storage system and the other is dry storage system. In the wet storage system, the spent fuels are placed inside the chemically controlled water pool located in the reactor building. Water is very efficient to cool down the decay heat and to shield the radiation coming from the spent fuels. However, a major problem is its limitations in space and difficulties of maintaining safe water chemistry environment. Whereas, dry storage system can store spent fuels far from the NPP and provide sufficient space. The dry storage system provides long-term storage about 40 years to safely confine the spent fuel from any external events such as earthquake, fire, or flood and to assure integrity of fuel cladding with ample safety margin. Therefore, to ensure the integrity

* Department of Nuclear Engineering, Hanyang University, Seoul 04763, Republic of Korea
† 교신저자(Corresponding Author), E-mail : sungjkim@hanyang.ac.kr

over long storage period, thorough investigation of safety parameters should be performed. Development of a dry storage system in Korea is underway due to saturation expected in interim spent fuel pool located in the NPPs in 5 to 10 years.

To compensate the limitations of wet storage system, the dry storage system necessitates adopting passive decay heat cooling mechanism, which is the natural convection by backfill gas inside the canister. Natural convection by gas can be realized through the buoyancy-induced flow, which strongly depends on thermo-physical properties of the working fluid and flow geometry. Several gases were suggested as backfill gas of the spent fuel dry storage system such as helium, air, nitrogen, and argon. Their properties show virtual difference, from which it can be expected that their natural convection characteristic inside the canister is likely to show some deviations. Note that in the current commercial design, canister is mainly backfilled with helium gas.

There are many researches reported regarding the dry storage system. S. Q. Shi et al.[1] studied on the hydrogen concentration limit and delayed hydride cracking of fuel cladding during dry storage and suggested the critical temperature limit. M. Keyhani et al.[2] suggested an empirical correlation based on experimental data between Nusselt number (Nu) and Rayleigh number (Ra) in a vertical rod bundle. Also, S. H. Yoo et al.[3], W. K. In et al.[4], L. E. Herranz et al.[5] conducted CFD studies inside the dry storage system. However, these studies investigated only in helium or air environment and no study has yet been focused on the difference of natural convection flow characteristics with different gases such as nitrogen or argon and their cooling capability inside the spent fuel dry storage system even though they are frequently used as coolant in other applications.

Thus, the objective of this study is to utilize CFD code to compare the inherent characteristics of natural circulation with four kinds of possible working fluids, helium, air, nitrogen, and argon gases inside the canister of spent fuel dry storage system. Peak cladding temperature (PCT), Reynolds number for each sub-channel, and z-vector velocity contour were compared for all explored cases. Results were compared with the empirical correlation developed with

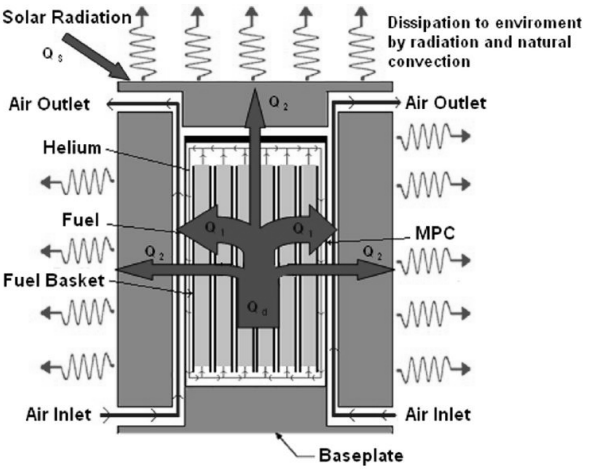

Fig. 1 Conceptual design of dry storage system

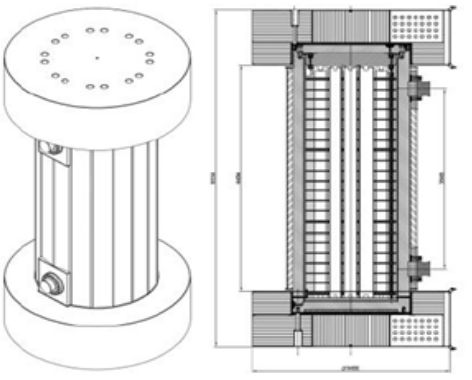

Fig. 2 Dry Storage system designed for transportation and storage in Korea

experimental data by M. Keyhani et al.[2] and vertical wall laminar natural convection flow correlation suggested by Chu and Churchill[6] for validation. CFD analysis was conducted with ANSYS FLUENT 17.0 based on some assumptions to save the computational costs and detailed information is presented in Section 3.

2. Description of Spent Fuel Dry Storage System

There are various types of spent fuel dry storage system model such as TN-24P cask, HI-STORM100S, which are frequently studied in many countries. These dry storage system models are designed to contain 21 to 32 spent fuel assemblies in one system. Typically, a dry storage system consists of concrete cask and stainless steel canister containing the fuel assemblies transported from the spent fuel pool and it is put inside the concrete cask. Fig. 1 and 2 show the

Table 1 Dimensions of canister and concrete cask

	Canister	Concrete Cask
Outer Length	4.88 m	6.18 m
Inner Length	4.58 m	4.93 m
Inner Diameter	1.636 m	1.866 m
Wall Thickness	25 mm	700 mm

conceptual design showing heat transfer mechanisms in the dry storage system and the dry storage system design for the localization to store 21 spent fuel assemblies, respectively. Natural convection flow occurs inside the canister and air channel between the canister and the cask. For this study, the model shown in Fig. 2, which is the dry storage system model for transportation and storage developing in Korea, was chosen and its dimensions of the canister and the concrete cask are listed in Table 1.

2.1 Thermo-physical Properties of the Backfill Gas inside the Canister

Backfill gas inside the canister is the front line coolant to cool down the decay heat. Thus, its essential requirement is the passive cooling capability. Also, for the long-term storage, it should be chemically stable not to react with the surrounding materials yielding oxidation and activation by radiation. Considering the abovementioned requirements, commercial designs adopted helium as the backfill gas of dry storage system because of its chemical inertness and high thermal conductivity and specific heat. Concurrently, other candidates for the backfill gas such as air, nitrogen, and argon were also suggested because they are frequently used as coolant in many applications.

Rayleigh number (Ra) is the governing factor that determines the natural convective flow characteristic defined below. Ra also can be rewritten as a product of Grashof number (Gr) and Prandtl number (Pr).

$$Ra = \frac{g\beta \Delta T L^3}{\nu\alpha} = Gr \cdot \Pr \quad (1)$$

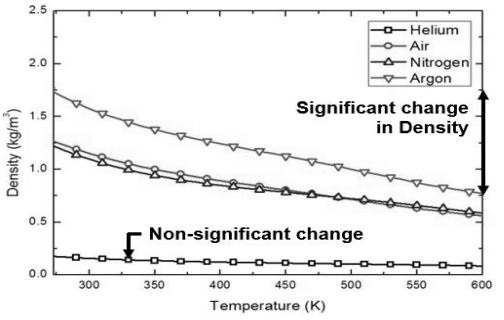

(a)

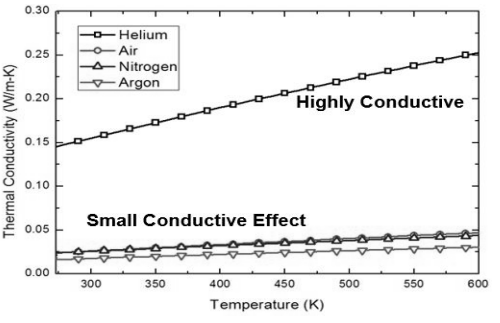

(b)

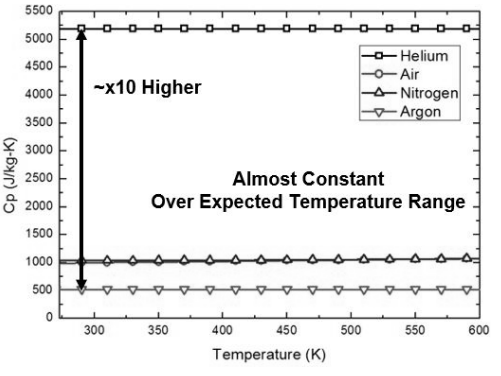

(c)

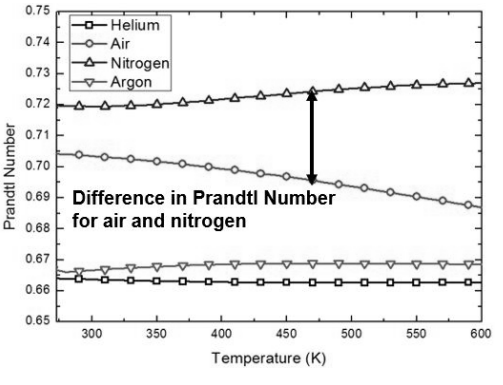

(d)

Fig. 3 (a) Density, (b) thermal conductivity, (c) specific heat (d) Prandtl number of fluids depending on temperature

Fig. 3 shows the comparison of density, thermal conductivity, specific heat, and Prandtl number (Pr) of four fluids, helium, air, nitrogen, and argon with respect to temperature. Significant difference is observed for helium with others. Helium shows almost no density change with temperature. It bears uniquely

high thermal conductivity and capability to contain heat about 10 times higher than that of argon. On the other hand, argon shows low conductive characteristic and cannot contain much heat even less than air or nitrogen. However, density change of argon per unit temperature is comparable to other fluids. Thus, some potential for producing buoyancy force is expected with argon. Air and nitrogen show very similar properties, which is understandable considering that air mostly consists of nitrogen. Nevertheless, despite of similar properties, air and nitrogen show different behavior in Prandtl number with temperature. Nitrogen shows increasing Prandtl number with temperature, from which natural convection is expected to show difference in high temperature region with air. For the evaluation of aforementioned characteristics, fluid property data were obtained from National Institute of Standards and Technology (NIST) chemistry webbook.

3. Numerical Modeling

In this study, a commercial CFD analysis tool, ANSYS FLUENT 17.0 was employed to explore the natural convective flow characteristic in the canister of dry storage system and to investigate the dominant heat removal mechanism with various backfill gases. The comparison of maximum cladding surface temperature inside fuel assembly, Reynolds number distribution of flow inside the sub-channels and investigation of relationship between Rayleigh number (Ra) and Nusselt number (Nu) were major interest in this study.

3.1 Assumptions for the Simulation

Simulating a full scale of spent fuel dry storage system is too expensive to perform. Therefore, to reduce the computational cost, following assumptions were considered.

1) Height was down-scaled by ratio of 1/2
2) Only a quarter of 16×16 fuel assembly was considered (8×8 partial assembly with a guide tube)
3) Flow area was adjusted by scaling law for single phase natural circulation system[7]
4) Radiative heat transfer is negligible

Radiative heat transfer cannot be neglected in full-scale simulation of dry storage system due to high surface temperature. However, for only one partial assembly, temperature difference between fuel rods and inner canister wall is insignificant to affect the total heat transfer.

3.2 Description of the Reference Fuel

The reference fuel for the simulation was selected as typical PWR fuel, which was cooled in the spent fuel pool for 1,000 days after the discharge with burnup of 45 GWD/MTU. Resulting decay heat was calculated as 6.25 W/rod.[8] GUARDINAN type 16×16 fuel assembly was adopted as the prototypical spent fuel assembly. Table 2 shows the general information about the GUARDIAN type fuel and its assembly.

Table 2 General information of GUARDIAN type fuel

Fuel rod diameter (mm)	9.7
Fuel rod length (m)	4.094
Effective length (m)	3.810
Fuel rod pitch (mm)	12.85
# of fuel rod/FA	236
Hydraulic diameter of sub-channel (mm)	11.97

3.3 Modeling of the Canister

Fig. 4 shows a schematic of the side and cross-sectional view of modeled geometry with dimensions. For simplicity, the canister shape was modified to square type and only a quarter of 8×8 partial assembly was considered assuming symmetry. There exists five distinct regions. Regions 1 and 2 indicate the heated and plenum region of the fuel rods, respectively. Region 3 represents the fluid region, where natural convective flow occurs. Regions 4 and 5 indicate the canister and free air space, respectively. Thickness of the canister was conserved and free air space was modeled to apply convective boundary condition at the outer wall of the canister. Stainless steel grade 304 (SS304) was adopted for canister material. Small circles inside the assembly are the locations indicating center of respective sub-channel in diagonal and radial direction named as FD 1, 2, 3 and FR 1, 2, 3,

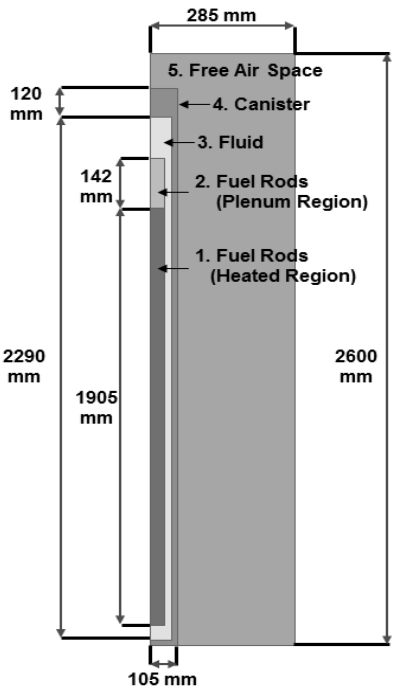

Fig. 4 Schematic of (a) side view, (b) Cross-sectional view of modeled geometry

respectively to extract data set.[3] Inner edge length of the canister was determined by following scaling law equation.[7] Ratio of flow area over inner area of the canister was matched between the model and the prototype.

$$A_{iR} = \frac{(a_i/a_0)_m}{(a_i/a_0)_p} = 1 \quad (2)$$

3.4 Grid Generation

The modeled geometry was meshed using ANSYS Mesh program as shown in Fig. 5. To reduce the number of high skewed cells generated near the narrow

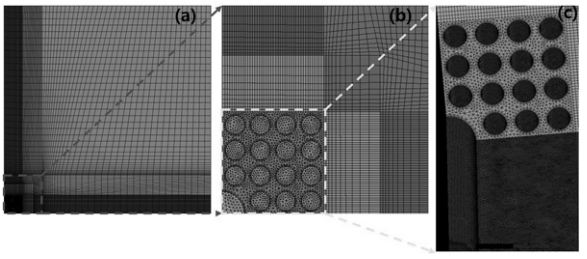

Fig. 5 Generated grids for (a) free air space, (b) canister, (c) fluid region

Table 3 FLUENT solver settings

Viscous Model Density Model		Laminar Boussinesq
Spatial Discretization	Gradient	Least Squares Cell Based
	Pressure	Body Force Weighted
	Momentum	1st Order Upwind
	Energy	1st Order Upwind
Pressure-Velocity Coupling		SIMPLE

gap between the fuel rods, small size tetrahedron cell was utilized. The grid system generated contains about 15,000,000 nodes and 30,000,000 cells with average skewness of 0.174 and average orthogonal quality of 0.93, which falls in a good quality range for simulation.

3.5 Solver Settings

After the grid generation step, the generated mesh file was imported to FLUENT 17.0. Solver settings for FLUENT 17.0 simulation are shown in Table 3. All explored simulations were calculated under steady-state and gravitational condition. Flow was assumed as laminar flow because decay heat is small in terms of sub-channel.

Moreover, several initial and boundary conditions were considered. Zero velocity and gauge pressure condition were assigned to inlet and outlet of free air space to set free, unhindered state. A no-slip condition was applied to the fuel rods, guide tube, and walls of the canister. A symmetry condition was used at two side boundary surfaces adjacent to the guide tube. A coupled condition was utilized at fluid-solid interfaces. Bottom wall of the canister, plenum region of fuel rods, and side walls of free air space were

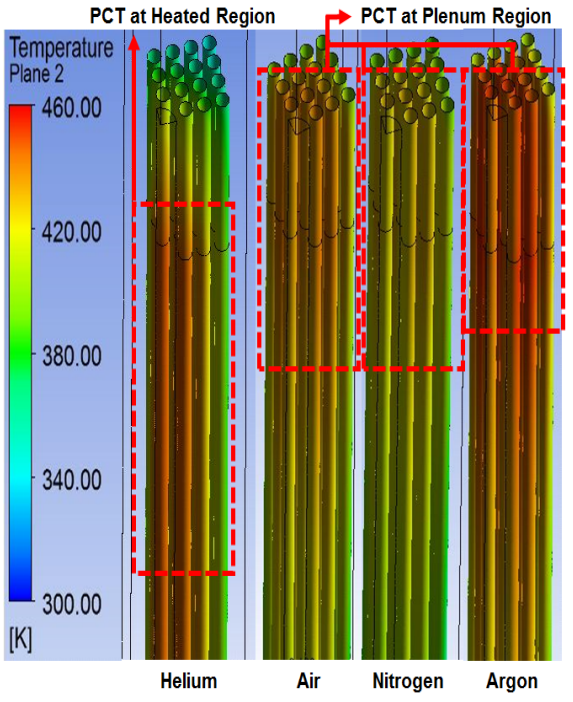

Fig. 6 Relative location of PCT for each case

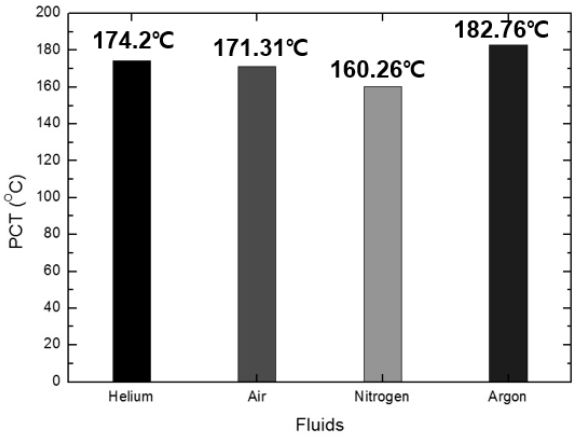

Fig. 7 PCT value for each case

applied with adiabatic condition. Heated region of the fuel rod was applied with constant heat flux of 53.83 W/m^2, which correspond to 6.25 W decay heat.

4. Results and Discussions

ANSYS FLUENT allows the users to investigate the flow motion of the working fluid inside the canister by solving the governing equations numerically. All the explored simulation cases continued until continuity and momentum residuals converged below 1×10^{-3} and energy residual below 1×10^{-7}.

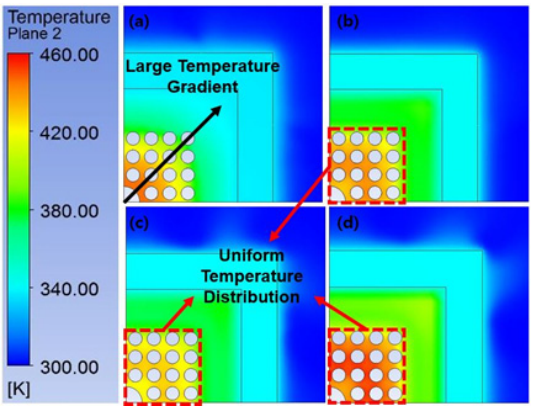

Fig. 8 Cross-sectional temperature distribution for (a) helium (b) air, (c) nitrogen, (d) argon at interface of plenum and heated region of the fuel rod

4.1 Peak Cladding Temperature (PCT)

Cladding surface temperature is a useful parameter to check out the effectiveness of natural convection heat removal by the backfill gas and cladding integrity. In addition, elevated location of PCT can be interpreted as higher axial heat transfer efficiency indicating effective buoyancy induced flow. Fig. 6 and 7 shows the PCT location for each case and its PCT value.

Argon gas shows the highest PCT followed by helium, air, and nitrogen. Also, while air, nitrogen, and argon cases show PCT at the plenum region of the fuel rod, PCT for helium is located under the plenum region, which indicates that helium does not have good axial heat transfer capability unlike the others. In addition, difference in temperature distribution inside the fuel assembly is significant as shown in Fig. 8. Temperature distribution is relatively uniform for air, nitrogen, and argon while helium shows large temperature gradient.

4.2 Axial Reynolds Number Distribution

Reynolds number is a decisive parameter to evaluate the inertia force against viscous force inside the flow channel. Fig. 9 shows the axial Reynolds number distribution along the axial direction from inlet (z=0 m) to outlet (z=2.047 m) of FD and FR direction sub-channels. Axial Reynolds number distribution inside the sub-channels can indicate how strong the natural convection flow occurs.

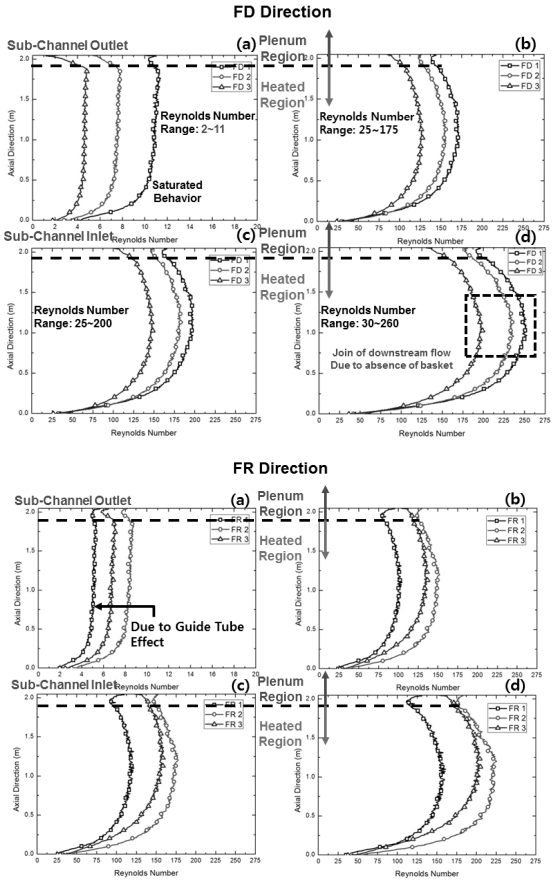

Fig. 9 Axial Reynolds number distribution along the sub-channels for (a) helium, (b) air, (c) nitrogen, (d) argon

As expected from Section 4.1, helium shows very weak axial flow compared to the others and Reynolds number ranges from 2 to 11. Also, Reynolds number showed saturated behavior in helium case while the other cases showed the peak because of joining of downstream flow due to absence of the basket. Argon showed the highest overall Reynolds number range. Nitrogen showed similar behavior with air with slightly higher Reynolds number range.

Assumption for laminar flow was validated considering Reynolds number range for all cases. Transition of flow regime into turbulent flow needs about 10 times higher flow velocity inside the sub-channels.

4.3 Z-vector Velocity Distribution

With the results from Sections 4.1 and 4.2, comparing the z-vector velocity distribution indicate how much heat is transferred to the outside of canister by checking the air velocity in the common region for

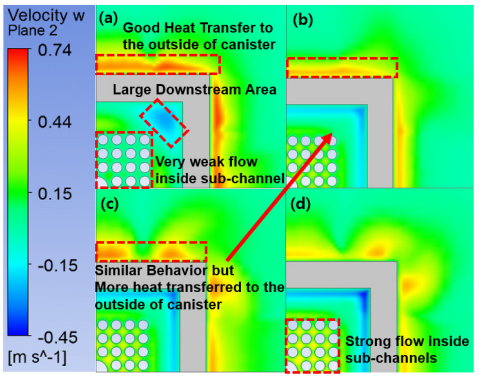

Fig. 10 Cross-sectional Z-vector velocity distribution for (a) helium, (b) air, (c) nitrogen, (d) argon at the interface of plenum and heated region of the fuel rod

all cases, free air space. Fig. 10 shows the cross-sectional contour of z-vector velocity distribution for each fluid. For helium, fast air movement is observed near the outside wall of the canister, which means most of the heat is transferred in radial direction. Air and nitrogen show similar contour but nitrogen transfers more heat to outside. Argon does not transfer much heat to the outside air even though the strongest flow is observed inside the canister.

4.4 Discussions on the Results

From the results of PCT, axial Reynolds number distribution, and z-vector velocity distribution, some significant differences were identified as follows.

1) Helium case showed the second highest PCT located under the plenum region with very low Reynolds number range and fastest air movement was observed at the free air space near the canister outside wall. These results indicate that most of the heat is transferred radially rather than axially by means of conduction. Also, even though helium has very high specific heat, its temperature distribution shows that heat is not removed very effectively compared to air or nitrogen. Compared with air and nitrogen cases, some limitation in convective heat transfer could be be seen for helium.
2) As for air and nitrogen cases, trend of results were very similar to each other. However, nitrogen shows the stronger natural convective

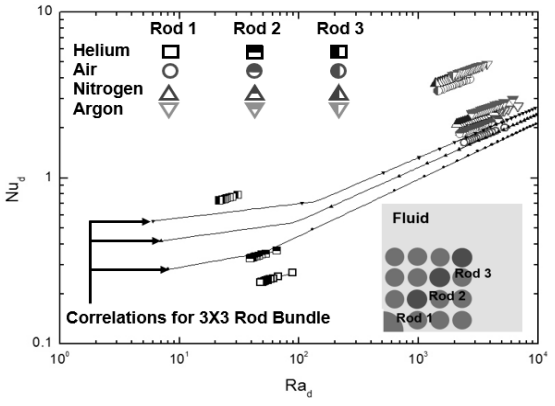

Fig. 11 Comparison of convective Nusselt number for the specific rod with empirical correlation

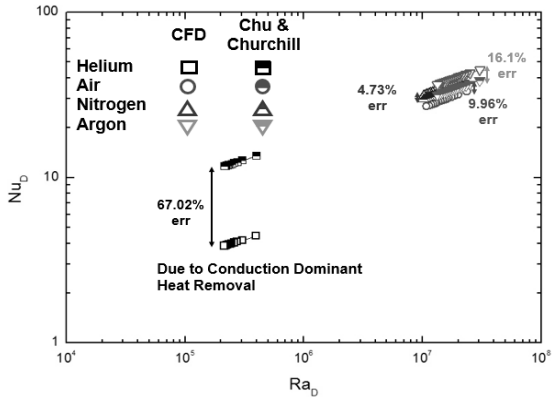

Fig. 12 Comparison of overall convective Nusselt number with correlation for vertical wall laminar natural convection

flow with much lower PCT inside the canister and faster air movement outside the canister. Due to difference shown in Prandtl number in Fig. 3, nitrogen shows the more effective natural convection and heat removal than other gases.

3) Argon showed the strongest natural convective flow. However, at the same time, PCT was the highest among the explored four fluids. Effective natural convective flow was expected form the substantial change in density with temperature but due to very low specific heat and thermal conductivity, argon could not contain the heat removed from the surface nor transfer the heat to the outside of canister.

4.5 Comparison with the Correlations

Simulation results were validated by comparing the results with empirical correlation with 3×3 rod bundle experiment data suggested by M. Keyhani et al.[2] and correlation for laminar natural convective flow at vertical plate suggested by Chu and Churchill.[6] Specific definition of parameters are listed in the nomenclature section.

Fig. 11 shows the correlation between Nusselt number (Nu_{di}) with Rayleigh number (Ra_{di}) based on diameter of the fuel rod defined in the referred study.[2] There are some errors due to geometric difference and size of fuel bundle. Also, the experiment was conducted only with helium and air backfilled condition. However, CFD simulation results show the similar trend to the empirical correlation.

Simulated cases are very different from vertical wall condition suggested by Chu and Churchill. However, assuming fuel assembly as the heated wall, its trend can be deemed as vertical wall with total heat source of 375 W. Overall convective Nusselt number was compared with that defined by the vertical wall correlation defined in Eqs. (3) and (4) using the Rayleigh number based on diameter of the canister (Ra_D) as shown in Fig. 12. The result with helium does not match very well as the average error was estimated about 67.02 %. This could be expected from the fact that heat is mostly removed by conduction. Argon case shows average error of 16.10 %, which is much less than helium. But due to low Prandtl number, effective natural convective flow could not be observed. Air and nitrogen cases are in good agreement with the correlation with average error of 9.96 % and 4.73 %, respectively. From this result, effective natural convective flow could be identified for air and nitrogen compared to helium or argon.

$$\psi = \left[1+\left(\frac{0.492}{\mathrm{Pr}}\right)^{9/16}\right]^{-16/9} \tag{3}$$

$$\overline{Nu_D} = 0.68 + 0.670\left(Ra_D\psi\right)^{1/4} \tag{4}$$

5. Conclusion

In this study, natural convective flow simulations for the various backfill gases for the canister of dry storage system were carried out using ANSYS FLUENT code. Helium, air, nitrogen, and argon were selected for the working fluids. Using the scaling law, 1/2

down-scaled geometry was modeled with same initial and boundary conditions. The major findings observed can be summarized as follows.

1) Helium gas showed low axial heat transfer efficiency and high PCT inspite of relatively high thermal conductivity and specific heat. Very weak flow was observed inside the sub-channel with Reynolds number less than 12 while fast air movement was observed at the outside of the canister. Thus, the heat is mostly transferred radially rather than axially for helium in form of conduction. Also, simulation result was not in good agreement with the existing natural convection correlation.
2) Air and nitrogen showed very similar behaviors to each other. However, even though air mostly consists with nitrogen, difference in Prandtl number was observed and thus nitrogen showed more effective natural convection with higher Reynolds number and much lower PCT.
3) Argon showed the strongest flow inside the canister but its coolability was the worst among four fluids explored. Due to low specific heat and thermal conductivity, argon showed small Prandtl number, from which effective natural convective flow could be observed. Strong flow is caused only due to large buoyancy effect.

From the comparison work, effectiveness of natural convective heat removal and flow characteristics were identified for each fluid in thermal-hydraulic point of view. Despite the fact that air could oxidize the cladding surface in high temperature condition, nitrogen showed more effective natural convection even though its similarity with air. Simulation results suggest that experimental validation for the nitrogen is needed to investigate potential coolability other than currently commercially used helium. However, chemical stability of helium and activation of nitrogen by radiation need to be considered to determine the backfill gas for the canister of dry storage system.

Acknowledgments

This research was supported by the Radioactive Waste Management Technology Program of the Korea Institute of Energy Technology Evaluation and Planning (KETEP), funded by the Ministry of Trade, Industry & Energy, Republic of Korea. (No. 2014171020166A)

Nomenclature

g	Gravitational constant [m/s^2]
β	Isobaric thermal expansion coefficient
L	Characteristic length [m]
ν	Kinematic viscosity [m^2/s]
α	Thermal diffusivity (= $k/\rho C_p$) [m^2/s]
T	Temperature [K]
$\triangle T$	Characteristic temperature difference (= $T_{MR1} - T_{MC}$) [K]
Gr	Grashof number (= $g\beta L^3 \triangle T/\nu^2$)
Pr	Prandtl number (= $\mu C_p/k$)
μ	Dynamic viscosity [Pa-sec]
C_p	Specific heat [J/kg-K]
k	Thermal conductivity [W/m-K]
ρ	Density [kg/m^3]
a_i	Cross-sectional flow area inside the canister [m^2]
a_0	Cross-sectional inner area of the canister [m^2]
A_{iR}	Flow area ratio
d	Diameter of the fuel rod [m]
D	Diameter of the canister [m]
A_D	Inner surface area of the canister [m^2]
h_{di}	Convective heat transfer coefficient on the ith rod (= $Q_c/A_D(T_{MRi} - T_{MC})$, i=1, 2, 3)
h_D	Overall convective heat transfer coefficient (= $Q_c/A_D \triangle T$)
Nu_{di}	Convective Nusselt number on ith rod (= $h_{di}d/k$, i=1, 2, 3)
Nu_D	Overall convective Nusselt number (= $h_D D/k$)
Ra_{di}	Rayleigh number based on diameter of fuel rod i (= $g\beta d^3(T_{MRi} - T_{MC})/\alpha\nu$, i=1, 2, 3)
Ra_D	Rayleigh number based on diameter of the canister (= $g\beta D^3 \triangle T/\alpha\nu$)

Subscript

MR	Mean value on rod
MC	Mean value on canister
m	model
p	prototype

References

(1) Shi, S. Q., Shek, G. K., and Puls, M. P., 1995, "Hydrogen concentration limit and critical temperatures for delayed hydride cracking in zirconium alloys," Journal of Nuclear Materials, Vol. 218, No. 2, pp. 189~201.

(2) Keyhani, M., Kulacki, F. A., and Christensen, R. N., 1985, "Experimental Investigation of Free Convection in a Vertical Rod Bundle-A General Correlation for Nusselt Numbers," Journal of Heat Transfer, Vol. 107, No. 3, pp. 611~623.

(3) Yoo, S. H., No, H. C., Kim, H. M., and Lee, E. H., 2010, "CFD-assisted scaling methodology and thermal-hydraulic experiment for a single spent fuel assembly," Nuclear Engineering and Design, Vol. 240, No. 12, pp. 4008~4020.

(4) In, W. K., Kwack, Y. K., Kook, D. H., and Koo, Y. H., 2014, "CFD Simulation of Heat and Fluid Flow for Spent Fuel in a Dry Storage," Transactions of Korean Nuclear Society Spring Meeting, Jeju, Korea.

(5) Herranz, L. E., Penalva, J., and Feria, F., 2015, "CFD analysis of a cask for spent fuel dry storage: Model fundamentals and sensitivity studies," Annals of Nuclear Energy, Vol. 76, pp. 54~62.

(6) Churchill, S. W. and Chu, H. H. S., 1975, "Correlating equations for laminar and turbulent free convection from a vertical plate," International Journal of Heat and Mass Transfer, Vol. 18, No. 11, pp. 1323~1329.

(7) Ishii, M. and Kataoka, I., 1984, "Scaling laws for thermal-hydraulic system under single phase and two-phase natural circulation," Nuclear Engineering and Design, Vol.81, No. 3, pp. 411~425.

(8) Ade, B. J. and Gauld, I. C., 2011, "Decay Heat Calculation for PWR and BWR Assemblies Fueled with Uranium and Plutonium Mixed Oxide Fuel Unsing Scale," ORNL/TM-2011/290.